IEEE Photonics Journal
An IEEE Photonics Society Publication

Theoretical and Experimental Optimization of O-Band Multiwavelength Mixed-Cascaded Phosphosilicate Raman Fiber Lasers

Volume 3, Number 4, August 2011

J. Z. Wang
Z. Q. Luo
Z. P. Cai
M. Zhou
C. C. Ye
H. Y. Xu

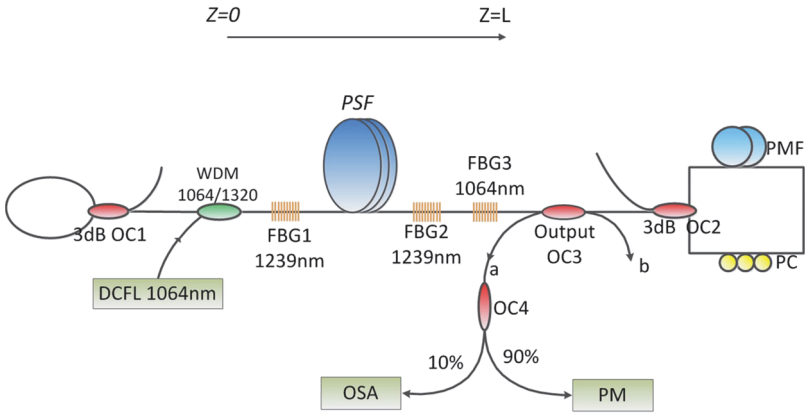

DOI: 10.1109/JPHOT.2011.2159263
1943-0655/$26.00 ©2011 IEEE

Theoretical and Experimental Optimization of O-Band Multiwavelength Mixed-Cascaded Phosphosilicate Raman Fiber Lasers

J. Z. Wang, Z. Q. Luo, Z. P. Cai, M. Zhou, C. C. Ye, and H. Y. Xu

Institute of Optoelectronic Technology, Department of Electronic Engineering, Xiamen University, Xiamen 361005, China

DOI: 10.1109/JPHOT.2011.2159263
1943-0655/$26.00 ©2011 IEEE

Manuscript received May 13, 2011; revised June 1, 2011; accepted June 4, 2011. Date of publication June 9, 2011; date of current version June 28, 2011. This work was supported in part by the Fundamental Research Funds for the Central Universities (2010121057). Corresponding author: Z. Q. Luo (e-mail: zqluo@xmu.edu.cn).

Abstract: We theoretically analyze and experimentally optimize an O-band mixed-cascaded multiwavelength phosphosilicate Raman fiber laser (MRFL). The theoretical analyses show that the output power is insensitive to the variation of Raman fiber length when it exceeds the optimal length. However, the pump threshold, slope conversion efficiency, and output power of the mixed-cascaded MRFL strongly depend on the output coupling ratio of the output optical coupler. When a 1064-nm Yb^{3+}-doped double-clad fiber laser is used to pump a section of phosphosilicate fiber (PSF) in a mixed-cascaded Raman cavity, both the Raman gains of P_2O_5 and SiO_2 in the fiber are utilized, and multiwavelength lasing around 1320 nm with a wavelength spacing of 0.8 nm has been obtained. The different coupling output ratios and Raman fiber lengths are used to optimize the output performances of the O-band mixed-cascaded MRFL. The maximum output power of the O-band MRFL is 1.3 W with the coupling output ratio of 80% and the PSF length of 1 km. The experimental results are in good agreement with the theoretical ones.

Index Terms: Multiwavelength fiber laser, mixed-cascaded, phosphosilicate, stimulate Raman scattering, optimization.

1. Introduction

O-band (~1310 nm) fiber lasers have attracted much attention due to their great potential applications in optical fiber communication systems, medicine, and astrophysics. For optical fiber communication systems, the O-band locates at the second optical communication window with low dispersion in the standard single-mode fibers. Especially, with the fast development of wavelength-division-multiplexing (WDM) technology, the O-band laser sources can be successfully applied in access network and metro system. For example, bidirectional communication access systems are commonly established by coarse 1310/1550-nm WDM technology [1]. However, the existing rare-earth-doped fiber lasers cannot cover the O-band [2]. Although one can use semiconductor optical amplifier (SOA) to operate at O-band [1], [3], [4], most SOA-based fiber lasers provide very low output power and are sensitive to environmental changes, which imposes some constraint in practical applications. In contrast, the stimulated Raman scattering (SRS) lasers have some fundamental advantages, such as (1) the lasing waveband can be arbitrarily chosen by adjusting the pump wavelengths; (2) relatively broad gain bandwidth [5]; (3) the Raman saturated output

power can be very high. Benefiting from these advantages of Raman amplifier, one can even realize an O-band multiwavelength fiber laser which could find some applications in dense WDM systems.

Most research on multiwavelength Raman fiber lasers has focused on the operation of C- or L-band [6]–[9]. The early multiwavelength Raman fiber lasers (MRFLs) usually used an array of semiconductor laser diodes (LDs) as the Raman pump sources [7], [8]. It is better to use a high-power Yb^{3+}-doped double-clad fiber laser (YDCFL) as the Raman pump which can make a MRFL more compact and low cost. By utilizing a 1064-nm YDCFL as the Raman pump and cascaded long-period fiber gratings as the comb-like filter, Han *et al.* [6] have reported an L-band MRFL with seven-order Raman shifts of SiO_2/GeO_2. When a 10 W/1064-nm YDCFL is used to pump three different kinds of Raman gain fibers, Kim *et al.* [9] have successfully presented S- and C-band MRFLs with a polarization-maintaining fiber (PMF) Sagnac loop mirror as the comb-like filter. However, most of SiO_2/GeO_2 MRFLs required many Raman-cascaded orders [6], [9], [10] for obtaining the desired lasing wavelength due to the small Raman frequency shift ($\sim$440 cm^{-1} only) of SiO_2/GeO_2, leading the complexity and high cost of the MRFLs. To reduce the number of Raman-cascaded orders, a feasible solution is to use the larger Raman shift ($\sim$1330 cm^{-1}) of P_2O_5 in P-doped fiber instead of the SiO_2/GeO_2 Raman shift. Unfortunately, due to the narrow gain bandwidth of the P_2O_5 SRS, it is difficult for the multiwavelength generation using Raman gain of P_2O_5 only.

Recently, we proposed a new mechanism for generating multiwavelength O-band lasing by combining the advantages of the large Raman frequency shift of P_2O_5 and the broadband Raman gain bandwidth of SiO_2/GeO_2 from the same phosphosilicate fiber (PSF). We experimentally achieved multiwavelength lasing in the O-band using a two-mixed-cascaded Raman PSF cavity pumped by a 1064-nm YDCFL [11]. However, only 3% power conversion efficiency was obtained from this structure because the O-band MRFL system was not optimized. It is very important to obtain the higher conversion efficiency and greater lasing number by optimizing the laser parameters of the MRFL. In this paper, by applying the fast and stable Newton–Raphson algorithm [12] to solve the Raman coupled-wave equations of mixed-cascaded O-band MRFL, we numerically analyzed the influences of the Raman fiber length and output coupling ratio on the conversion efficiency, the threshold pump power as well as the total output power. Then, based on the theoretical optimization, we experimentally designed the two-stage mixed-cascaded O-band MRFL and obtained an improved slope conversion efficiency of 33% and a maximum output power of 1.3 W.

2. Principle and Theoretical Model of O-band Mixed-Cascaded MRFL

It is well known that there are two frequency-shift peaks in the Raman spectrum of PSF, which originates from the Raman scatterings of SiO_2/GeO_2 and P_2O_5, respectively. For the PSF used in our experiment, the Raman scattering spectrum is showed in Fig. 1 [13]. One can find that the Raman scattering of P_2O_5 and SiO_2/GeO_2 have their respective features: 1) The Raman scattering of P_2O_5 has a large Raman frequency shift of 1327 $cm^{-1}$with a very narrow bandwidth; 2) the Raman scattering of SiO_2/GeO_2 has an ultrabroad bandwidth ($\sim$300 cm^{-1}), but its Raman frequency shift is relatively small ($\sim$495 cm^{-1} only). Considering their applications in MRFLs, the SRS of P_2O_5 has a great potential to reduce the Raman-cascaded orders, however, it is unsuitable to generate multiwavelength oscillation due to its narrow bandwidth. On the other hand, the ultrabroad Raman gain bandwidth of SiO_2/GeO_2 is advantageous for producing multiwavelength oscillation, but it will need more cascaded orders due to its small Raman frequency shift. Using the SRS of both P_2O_5 and SiO_2/GeO_2 in a PSF simultaneously, mixed Raman-cascaded MRFLs have been realized with only few cascaded orders [11]. The mixed Raman-cascaded process should meet the following design rules: 1) Because of the lack of narrow Raman gain bandwidth of P_2O_5, the last-order Raman shift for generating multiwavelength must utilize the SRS of SiO_2/GeO_2 benefiting from its ultrabroad bandwidth; 2) to reduce the Raman-cascaded orders for simplifying system, the SRS of P_2O_5 should be used as many times as possible. Complying with the above

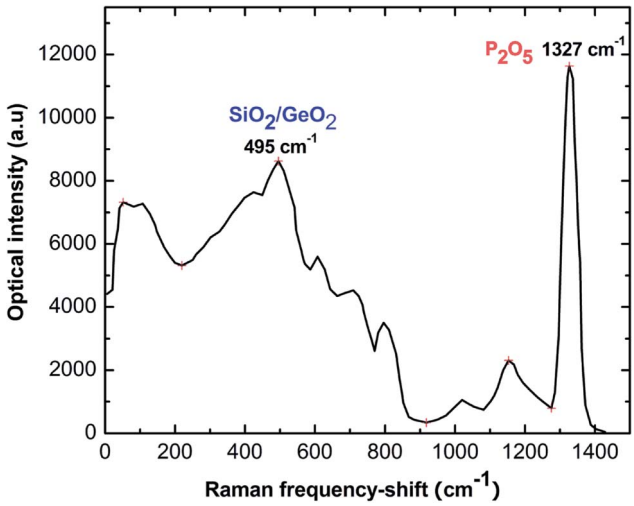

Fig. 1. Raman scattering spectrum of the phosphosilicate fiber [13].

rules, the proposed mixed-cascaded Raman process for realizing phosphosilicate MRFL can be described in principle by the following equations:

$$\begin{aligned}
&\frac{1}{\lambda_1} = \frac{1}{\lambda_p} - \Delta\nu_2 \\
&\vdots \\
&\frac{1}{\lambda_{n+1}} = \frac{1}{\lambda_n} - \Delta\nu_2 \\
&\vdots \\
&\frac{1}{\lambda_{N+1}^{out}} = \frac{1}{\lambda_N} - \Delta\nu_1
\end{aligned} \tag{1}$$

where λ_p is the pump wavelength; λ_n $(n = 1, 2, \ldots)$ is the nth-order Stokes wavelength; and λ_{N+1}^{out} $(N \geq n)$ is the central wavelength of the desired multiwavelength oscillation. $\Delta\nu_1$ and $\Delta\nu_2$ represent the Raman frequency shifts of SiO_2/GeO_2 and P_2O_5, respectively. For example, with the pump of 1064 nm, the first- and second-order Stokes waves can use the Raman frequency shift of P_2O_5 (oscillate at 1239 nm) and SiO_2/GeO_2 (oscillate at 1320 nm) to realize an O-band MRFL, respectively.

Fig. 2 shows the principle schematic of O-band multiwavelength mixed-cascaded phosphosilicate Raman fiber laser. A 1064-nm laser is used to pump a section of PSF for providing Raman gain. FBG1 and FBG2 are highly reflective at the first-order Stokes wave 1239 nm. The 3-dB OC1 forms a highly reflective loop mirror at the second-order Stokes wave, while the 3-dB OC2 combine a section of PMF and a PC to form a comb-like filter [9]. Then the OC3 outputs a partial second-order Stokes power to obtain multiwavelength laser at 1320 nm. An additional grating (FGB3) centered at pump wavelength for fully using the residual pump power. At this configuration, since the lengths of these optical devices (including OCs, FBGs, PC, PMF, and WDM) are much shorter than the Raman fiber, the whole cavity length can be simply equivalent to the length (L) of PSF.

Here, the two-stage mixed-cascaded MRFL can be governed by the following steady-state equations as

$$\frac{dP_0^{F/B}}{dz} = \mp\alpha_0 P_0^{F/B} \mp \frac{\nu_0}{\nu_1} g_1 \left(P_1^F + P_1^B\right) P_0^{F/B}$$

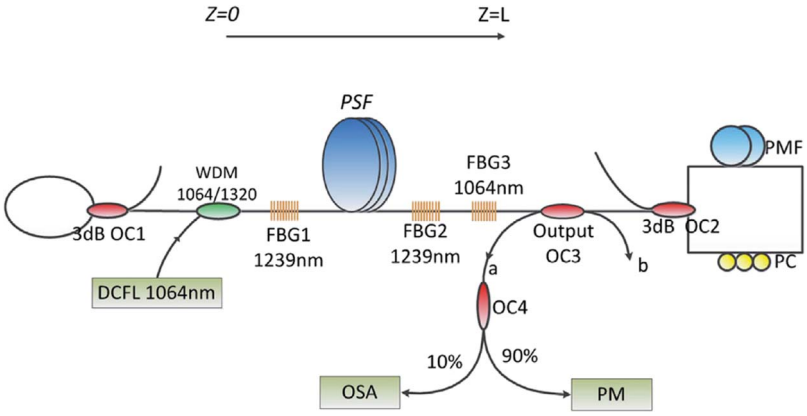

Fig. 2. Configuration of two-mixed-cascaded O-band MRFL.

$$\frac{dP_1^{F/B}}{dz} = \mp\alpha_1 P_1^{F/B} \pm g_1\left(P_0^F + P_0^B\right)P_1^{F/B} \mp g_2\frac{\nu_1}{\nu_2}\left(P_2^F + P_2^B\right)P_1^{F/B}$$

$$\frac{dP_2^{F/B}}{dz} = \mp\alpha_2 P_2^{F/B} \pm g_2\left(P_1^F + P_1^B\right)P_2^{F/B} \tag{2}$$

where the superscript, "F" and "B" denote the forward- and backward-propagation directions of pump or Stokes waves, respectively. P_0, P_i $(i = 1, 2)$ represent the pump power, ith-order Stokes wave power, and ν_0, ν_i $(i = 1, 2)$ are the corresponding optical frequencies. α_0, α_i $(i = 1, 2)$ are the coefficients of the fiber loss at the pump and Stokes wavelengths. The parameters g_i $(i = 1, 2)$ are the corresponding Raman gain coefficients of P_2O_5 and SiO_2/GeO_2. In (2), we neglect the contribution of spontaneous Raman scattering once the Raman oscillation happens. The boundary conditions for the mixed-cascaded MRFL are given by the reflection of the mirrors and the injected pump power

$$\begin{aligned} &P_0^F(0) = P_{\text{in}}, && P_0^B(L) = R_0^L \cdot P_0^F(L) \\ &P_1^F(0) = R_1^0 \cdot P_1^B(0), && P_1^B(L) = R_1^L \cdot P_1^F(L) \\ &P_2^F(0) = R_2^0 \cdot P_2^B(0), && P_2^B(L) = R_2^L \cdot P_2^F(L) \end{aligned} \tag{3}$$

where R_0^L is the reflection of the FBG3 at pump power, R_1^0 and R_1^L are the reflectivity of the FBG1 and FBG2 at z = 0 and z = L, respectively. R_2^0 and R_2^L represent the reflectivity of the OC1 broadband mirror and the PMF Sagnac loop mirror at z = 0 and z = L, respectively.

To solve (2) and (3), the two-point boundary problem must be transferred into an initial-value problem, and the correct initial values P_i^B $(i = 0, 1, 2)$ should be obtained firstly. Many researchers have numerically simulated the normal Raman fiber lasers using some different methods [14]–[18]. We apply a fast and stable algorithm in [12] which can reduce the calculating time to a few minutes. The basic idea of the fast algorithm can be simply described in the next. At the beginning, (3) can be transformed to following equations:

$$\begin{aligned} &P_0^F(0)/P_{\text{in}} = 1, && P_0^B(L)/P_0^F(L) = R_0^L \\ &P_1^F(0)/P_1^B(0) = R_1^0, && P_1^B(L)/P_1^F(L) = R_1^L \\ &P_2^F(0)/P_2^B(0) = R_2^0, && P_2^B(L)/P_2^F(L) = R_2^L. \end{aligned} \tag{4}$$

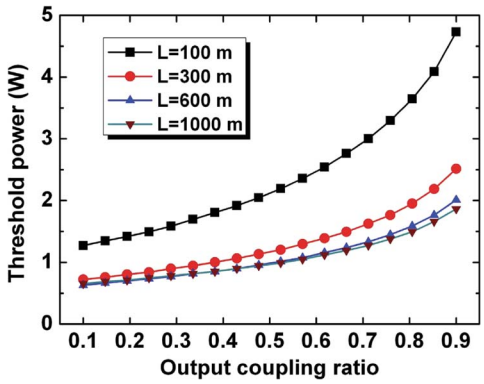

Fig. 3. Calculated threshold versus output coupling ratio for different lengths of PSF.

One can find that P_i^F $(i = 0, 1, 2)$ and P_i^B $(i = 0, 1, 2)$ are correlated by the boundary condition (4). Moreover, $P_i^F(L)$ and $P_i^B(L)$ also actually depend on $P_i^F(0)$ and $P_i^B(0)$ by (2). Thereby, the two-point boundary problem can transfer to exactly obtain the set of initial values as follows:

$$P(0) = \left[P_0^B(0), P_1^B(0), P_2^B(0)\right]^T. \tag{5}$$

Simultaneously, the output function $Output(P(0))$ and the target output function $Targetouput(L)$ are also defined as

$$\begin{aligned} Output(P(0)) &= \left[P_0^B(L)/P_0^F(L), P_1^B(L)/P_1^F(L), P_2^B(L)/P_2^F(L)\right]^T \\ Targetoutput(L) &= \left[R_0^L, R_1^L, R_2^L\right]^T. \end{aligned} \tag{6}$$

Only when the output function $Output(P(0))$ is equal to the target function $Targetouput(L)$, the input initial values $P(0)$ are the correct ones. Otherwise, the input initial values $P(0)$ are need further modified by applying the Newton–Raphson method mentioned in [12].

3. Numerical Simulation and Raman Cavity Optimization

In this section, we perform the numerical simulation for the multiwavelength mixed-cascaded Raman fiber laser and try to find the optimization parameters (e.g., the optimized coupling output ratio and PSF length). In our simulation, the parameters of PSF are directly used those of the PSF provided by Fiber Optics Research Center of Russia. The fiber core contains 13 mol. % of phosphor, which results in a refractive index difference of 0.011. The cutoff wavelength is 1000 nm that guarantees the single-mode behavior at the pump and Stokes-wave wavelengths. For the 1064-, 1239-, and 1320-nm wavelengths, the fiber loss coefficients are $\alpha_0 = 1.84$, $\alpha_1 = 1.16$, and $\alpha_2 = 1.00$ dB/km, respectively. The Raman frequency shifts are $\Delta\nu_1 = 495$ cm^{-1} and $\Delta\nu_2 = 1327$ cm^{-1}. Their Raman gain coefficients (at 1060 nm pump) are $g_1 = 0.85$ and $g_2 = 1.20$ kW^{-1}m^{-1}. The reflectivity of all the FBGs are approximately 99% with a 3-dB bandwidth of about 1 nm. All the FBGs and optical couplers are assumed to have the average insertion losses of 0.15-dB, which include the absorption, scattering, and splicing losses generated in the fabrication process. The PMF Sagnac comb-like mirror can usually induce a larger loss which is assumed to be 3 dB. Considering these losses as mentioned in above, the equivalent reflectivity of second-order cavity can be estimated as $R_2^L = (1 - Ratio)^2 \times 0.425$ and $R_2^0 = 0.85$, where $Ratio$ represents the output coupling ratio of OC3. With these parameters, we can solve the ordinary nonlinear differential equations (2) in MATLAB using the algorithm mentioned in Section 2. As shown in Fig. 3, the threshold pump power is numerically calculated as a function of output coupling ratio under different lengths of PSF. The threshold increases either with increase of the output coupling ratio or with decrease of the PSF length from 1000 m to 300 m. To minimize the threshold, one can choose a

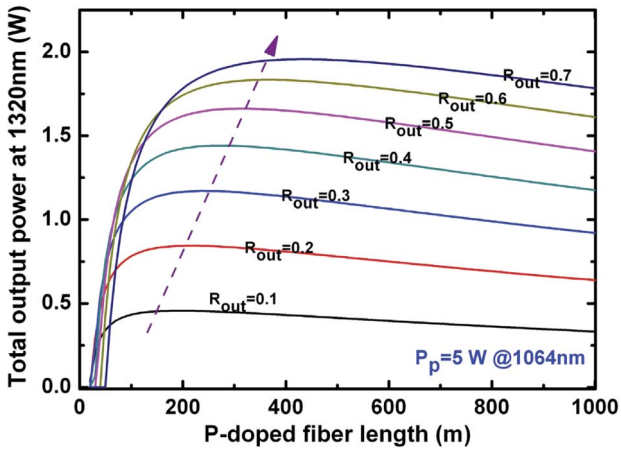

Fig. 4. Calculated total output power at 1320 nm versus PSF length for different output coupling ratios.

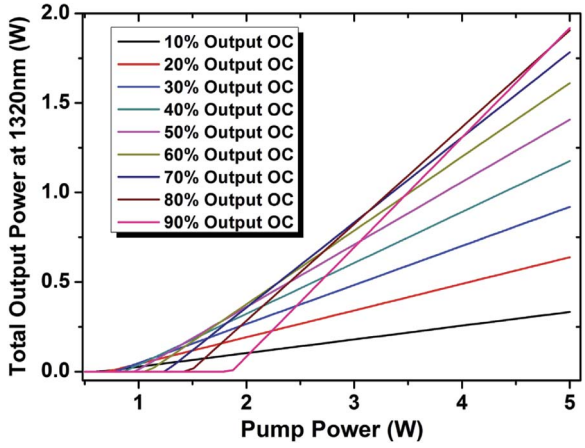

Fig. 5. Slope efficiency with different output coupling.

low output optical coupler and a long PSF. The calculated total output power of O-band (~1320 nm) is plotted against the PSF length for different output coupling ratios at a pump power of 5 W, as shown in Fig. 4. It is evident that the output power is insensitive to the variation of Raman fiber length when the length exceeds 300 m. Nevertheless, as shown in the dashed line of Fig. 4, the output coupling ratio can significantly influence on the output power and the optimal length (L_{opt}), for example, the $L_{opt} = 198$ m, $P_{out}^{max} = 0.45$ W for $R_{out} = 10\%$ and the $L_{opt} = 425$ m, $P_{out}^{max} = 1.95$ W for $R_{out} = 70\%$.

From both Figs. 3 and 4, one can find that the output coupling ratio has dominant effects to the threshold and conversion efficiency, while the PSF length is insensitive when it exceeds the optimal length. Therefore, we focus on the output coupling ratio to optimize the laser output of the mixed-cascaded MRFL. In practical design, one can usually use a longer PSF than the optimal length for reasonably ignoring the influence of Raman fiber length. In the next simulations, we adopt the 1000-m length of PSF (more than the optimal length).

Fig. 5 illustrates the slope efficiency of O-band lasing power with different output coupling ratios. It shows that the slope efficiency is in proportion to the output coupling ratio, but the threshold increases along with the coupling ratio which can observe from both Figs. 3 and 5. The minimum slope efficiency of 7.65% is obtained at $R_{out} = 10\%$ and the maximum slope efficiency of 61.2% is obtained at $R_{out} = 90\%$. However, it is not always a good choice to select the highest output

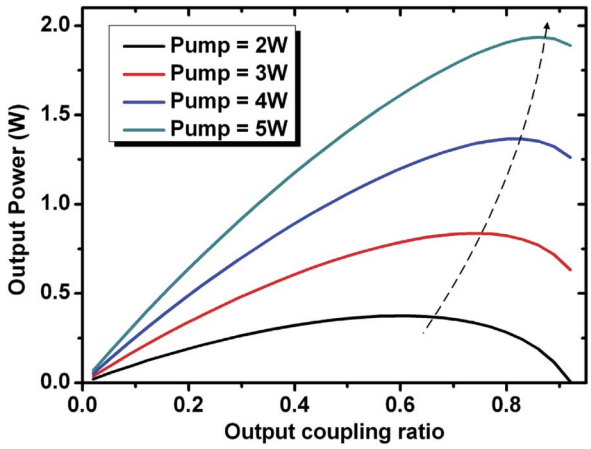

Fig. 6. Total output power verse output coupling ratio at 1320 nm with different pump power.

coupling ratio due to its high threshold and spectral characteristic. In fact, the optimal coupling ratio which can obtain the maximum output power will change with the variation of pump power. Fig. 6 shows the relationship between output coupling ratio and output power for different pump powers. The higher is the pump power, the larger output ratio is needed to obtain maximum output power. It can be estimated that the output power will reach maximum value at an output coupling ratio of ~90% when the pump power is greater than 5 W. In addition, the spectral characteristics will also be affected by the output coupling ratio, which will be discussed in the next section. As a result, we must select proper parameters to form an optimal laser configuration under the different conditions and applications.

4. Comparison With Experimental Results

Fig. 2 also shows the experiment setup of the proposed mixed-cascaded phosphosilicate MRFL. A commercial YDCFL (IPG-YLR-20-SM) with the output wavelength of 1064 nm and the output power up to 20 W is used as the Raman pump. The pump light was launched into the laser cavity through a 1064/1320 nm WDM. The first- and second-stage Raman cavities have been described in Section 3, and we adopt a ~5.5 m PMF ($\Delta n = 4.16 \times 10^{-4}$). The ports (a&b) of the output coupler (OC3) were used to extract the laser output from forward- and backward-propagation waves, respectively. In our experiment, the total output power represents the sum of two ports. An extra optical coupler (OC4) was used to simultaneously monitor the output spectrum and output power. The output laser spectrum was monitored by an optical spectrum analyzer (OSA) and the output power was measured by an optical power meter (PM). In Fig. 2, the PMF Sagnac loop filter operated at 1280 ~ 1340 nm was used as the comb-like wavelength selective element due to its advantages [9]. The channel spacing of its reflective or transmission spectrum can be calculated by

$$\Delta\lambda = \frac{\lambda^2}{\Delta n \cdot L_M} \tag{7}$$

where Δn and L_M denote the birefringence value and the length of PMF used in the filter, respectively. The channel spacing of the 5.5-m PMF Sagnac loop mirror can be calculated to be 0.8 nm. From (7), one can find that the channel spacing can be changed by varying the length of PMF. Moreover, it has been reported [9] that each peak wavelength in its reflective/transmission spectrum can be continuously tuned over a channel spacing by rotating the wave plates of PC in the Sagnac loop filter.

The output coupler (OC3) utilized in the experiment can be with different output coupling ratios (e.g., 20/80, 80/20, 30/70, 70/30, 40/60, 60/40). As increasing the pump power, the first-order

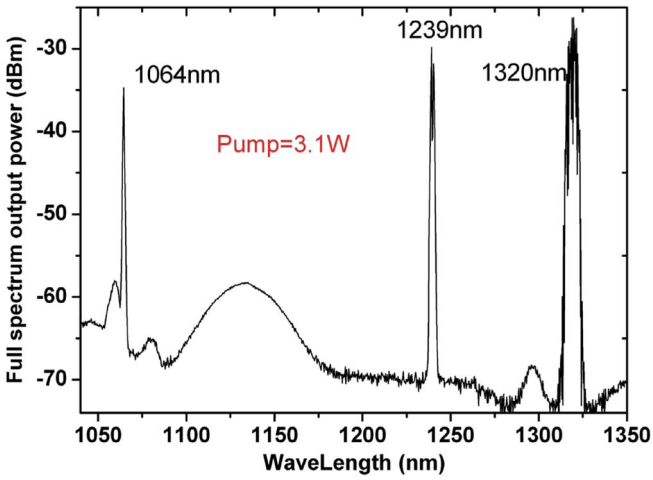

Fig. 7. Measured output spectrum of the MRFL, including the pump, first-, and second-order Stokes waves.

Stokes wave reaches its threshold and increases with pump power. Then, the first-order Raman laser is employed as the pump source of second-order Stokes wave. As further increasing pump power, the second-order Stokes wave occurs. Since all the FBGs have a small transmission of $\sim$1% at each central wavelength, the intracavity lasers at 1064 and 1239 nm have weak leakage at the output ports. Fig. 7 illustrates the whole spectrum of the Raman laser at the pump power of 3.1 W with a 30% output coupler. It can be clearly seen that 1239- and 1320-nm Stokes waves simultaneously oscillate in the Raman cavity, and the intensity of 1320-nm laser is obviously much stronger than the pump power and the first-order Stokes wave.

Using different output couplers, we record four different operation states of the MRFL with the almost same pump power as illustrated in Fig. 8. One can find from Fig. 8 that seven, six, five, and four lasing channels around 1320 nm are obtained with an optical coupler of output ratio 20%, 30%, 40%, and 60%, respectively. The wavelength spacing is 0.8 nm. The power nonuniformity and the extinction ratio are < 5 dB and > 25 dB, respectively. Moreover, the number of lasing channels can be further increased by boosting pump power [11]. It should be noted that the number of lasing channels is gradually reduced with increasing the output coupling ratio. It is understood that the increase of output coupling ratio introduces larger cavity loss, and reduces the lasing channel number. At the same time, using an OSA with a spectral resolution of 0.01 nm, we measure the 3-dB linewidth of each laser channel under different pump levels. With a pump power of 1.6, 2.0, 2.46, and 2.8 W, the measured linewidth are 0.227, 0.260, 0.284, and 0.292 nm, respectively. It is interesting to note that the 3-dB linewidth increases as increasing the pump power. This mainly is attributed to [19] 1) the narrow longitudinal mode spacing; 2) the strong four-wave-mixing (FWM); and 3) the spatial hole burning effect.

As shown in Fig. 9, the pump threshold of the MRFL were measured under different ratios of output optical coupler. The solid line and squares represent the numerical results and experimental data, respectively. The numerical results agree well with experimental data on the condition of the low output ratio, while the slight deviation happen in the case of high output ratio. It can be explained that the total loss estimated in the cavity is not accurate enough and the errors would be amplified with a larger output ratio.

Under different output coupling ratios, the measured total output power at $\sim$1320 nm is plotted against the input pump power, as shown in Fig. 10. A slope conversion efficiency of 33% and the maximum output power of 1.3 W have been obtained at a 80% output coupling ratio and a pump power of 5 W, which are significantly greater than the previous work [11]. We note that the measured slope efficiency is 10% at $R_{\text{out}} = 20\%$ and 33% at $R_{\text{out}} = 80\%$, while the corresponding numerical results are 15% at $R_{\text{out}} = 20\%$ and 54% at $R_{\text{out}} = 80\%$. The measured data do not well

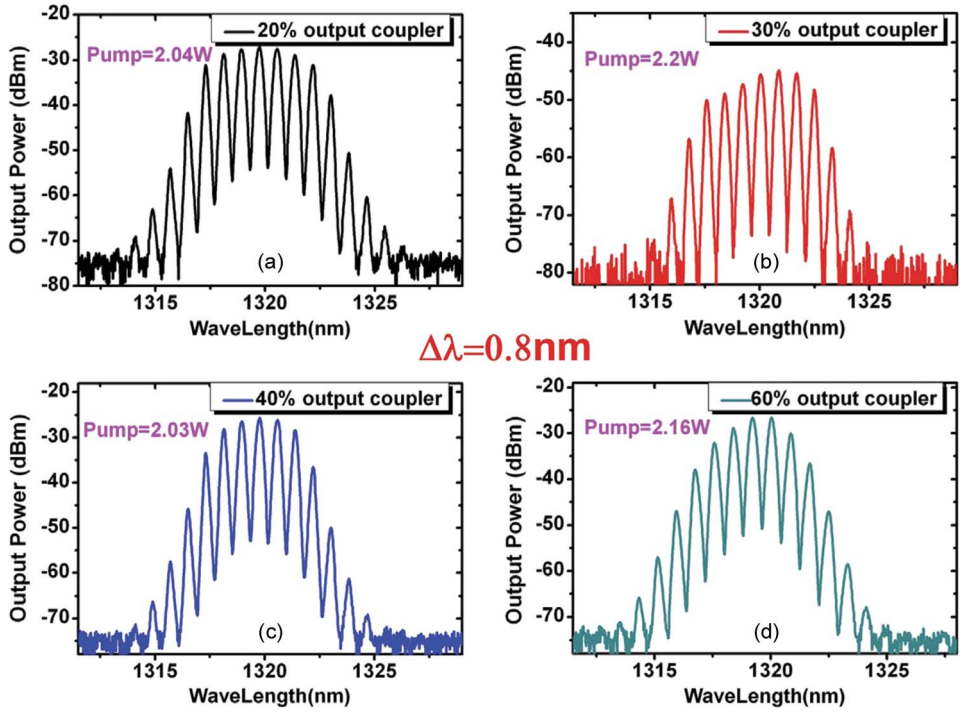

Fig. 8. Multiwavelength spectra for different output coupling ratios.

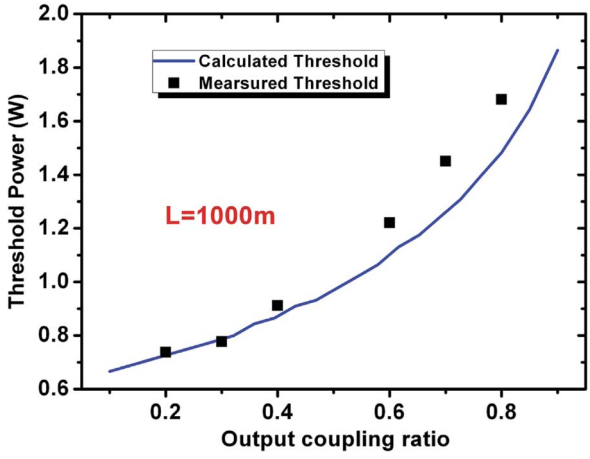

Fig. 9. Threshold as a function of output coupling ratio at L = 1000 m (Squares: Experimental data. Solid line: Numerical simulation).

coincide to the simulation results because the estimated total loss in our numerical model is not enough accurate. Additionally, as described in Fig. 4, the conversion efficiency is insensitive to the variation of PSF length after exceeding the optimal length. To testify this characteristic, Fig. 11 illustrates the slope conversion efficiency with different Raman fiber length at the output coupling ratio of 70%. It can be seen that the slope conversion efficiency is 22.5% for L = 1000 m and 28.5% for L = 350 m, where it is the optimal length at the $R_{out} = 70\%$, but the pump threshold is significantly increasing from 1.45 W at L = 1000 m to 3.29 W at L = 350 m, respectively.

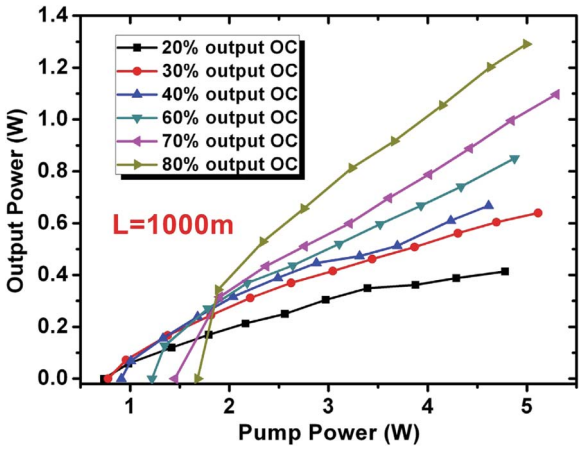

Fig. 10. Measured output power as a function of pump power.

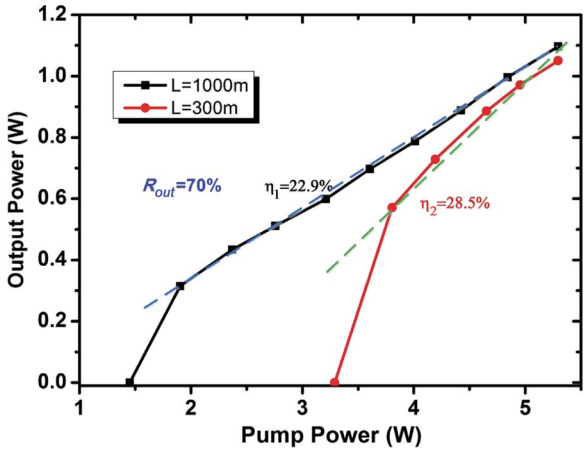

Fig. 11. Slope conversion efficiency for different lengths of PSF (1000 m and 350 m).

5. Discussions

According to the theoretical and experimental optimization in above, the design of O-band mixed-cascaded MRFL should take into account the following considerations.

1) The theoretical analyses show that the slope conversion efficiency of an O-band mixed-cascaded MRFL is insensitive to the variation of the Raman fiber length when it exceeds the optimal length. In contrast, the output coupling ratio has significantly influenced on both the threshold and conversion efficiency.
2) The numerical and experimental results indicate that a high output ratio of output optical coupler is required to obtain high conversion efficiency. As described in Fig. 5, with boosting the pump power, a ~90% output OC should be the optimal choice to get the maximum output power.
3) The number of lasing channels gradually decreases with increasing the output coupling ratio, as shown in Fig. 10.

In practice, for different applications, one may require different characteristics of the MRFL. Therefore, we briefly discuss how to achieve optimal structure for different applications. When a MRFL with high output power is required, using a high output coupling ratio (e.g., 80%, 90%), is a good choice. For optical fiber communication systems [20], it needs a stable MRFL with as many lasing channels as possible. For this purpose, one should adopt a lower output coupling ratio and a

longer PSF for obtaining a large number of lasing channels and a lower pump threshold. Meanwhile, it is also an alternate way by boosting the pump power for more lasing channels. In a word, for different applications, one should choose a proper optimal scheme for the desired applications.

6. Conclusion

We have numerically optimized the O-band multiwavelength mixed-cascaded phosphosilicate Raman fiber laser by applying the coupled-wave equations and the Newton–Raphson method. We also carried out experimental studies to testify the numerical results. The experimental results are in good agreement with the theoretical ones. We have demonstrated an O-band MRFL lasing around 1320 nm with a wavelength spacing of 0.8 nm, extinction ratio $>$ 25 dB and the power nonuniformity less than 5 dB. The maximum output power of the O-band MRFL is as high as 1.3 W with the coupling output ratio of 0.8 and the PSF length of 1 km. In addition, taking into account both the conversion efficiency and the number of lasing channels, we have discussed how one can obtain an optimum configuration of MRFLs in special applications.

References

[1] J. P. Turkiewicz, "Application of O-band semiconductor optical amplifiers in fibre-optic telecommunication networks," Ph.D. dissertation, Technische Univ. Eindhoven, Eindhoven, The Netherlands, 2006.

[2] I. A. Bufetov and E. M. Dianov, "Bi-doped fiber lasers," *Laser Phys. Lett.*, vol. 6, no. 7, pp. 487–504, Jul. 2009.

[3] H. Ahmad, M. Z. Zulkifli, A. A. Latif, and S. W. Harun, "Novel O-band tunable fiber laser using an array waveguide grating," *Laser Phys. Lett.*, vol. 7, no. 2, pp. 164–167, Feb. 2010.

[4] T. Sakamoto, T. Yamamoto, K. Kurokawa, and S. Tomita, "DWDM transmission in O-band over 24 km PCF using optical frequency comb based multicarrier source," *Electron. Lett.*, vol. 45, no. 16, pp. 850–851, Jul. 2009.

[5] M. N. Islam, "Raman amplifiers for telecommunications," *IEEE J. Sel. Topics Quantum Electron.*, vol. 8, no. 3, pp. 548–559, May 2002.

[6] Y. G. Han, C. S. Kim, J. U. Kang, U. C. Paek, and Y. Chung, "Multiwavelength Raman fiber-ring laser based on tunable cascaded long-period fiber gratings," *IEEE Photon. Technol. Lett.*, vol. 15, no. 3, pp. 383–385, Mar. 2003.

[7] Y. G. Han, S. B. Lee, D. S. Moon, and Y. Chung, "Investigation of a multiwavelength Raman fiber laser based on few-mode fiber Bragg gratings," *Opt. Lett.*, vol. 30, no. 17, pp. 2200–2202, Sep. 2005.

[8] Y. G. Han, J. H. Lee, S. B. Lee, L. Poti, and A. Bogoni, "Novel multiwavelength erbium-doped fiber and Raman fiber ring lasers with continuous wavelength spacing tunability at room temperature," *J. Lightw. Technol.*, vol. 25, no. 8, pp. 2219–2225, Aug. 2007.

[9] C. S. Kim and J. U. Kang, "Multiwavelength switching of Raman fiber ring laser incorporating composite polarization-maintaining fiber Lyot-Sagnac filter," *Appl. Opt.*, vol. 43, no. 15, pp. 3151–3157, May 2004.

[10] J. W. Nicholson, M. F. Yan, P. Wisk, J. Fleming, F. DiMarcello, E. Monberg, T. Taunay, C. Headley, and D. J. DiGiovanni, "Raman fiber laser with 81 W output power at 1480 nm," *Opt. Lett.*, vol. 35, no. 18, pp. 3069–3071, Sep. 2010.

[11] Z. Q. Luo, Z. P. Cai, J. Huang, C. C. Ye, C. Huang, H. Xu, and W. D. Zhong, "Stable and spacing-adjustable multiwavelength Raman fiber laser based on mixed-cascaded phosphosilicate fiber Raman linear cavity," *Opt. Lett.*, vol. 33, no. 14, pp. 1602–1604, Jul. 2008.

[12] Z. Q. Luo, C. C. Ye, G. Y. Sun, Z. P. Cai, M. L. Si, and Q. B. Li, "Simplified analytic solutions and a novel fast algorithm for Yb^{3+}-doped double-clad fiber lasers," *Opt. Commun.*, vol. 277, no. 1, pp. 118–124, Sep. 2007.

[13] E. M. Dianov, M. V. Grekov, I. A. Bufetov, S. A. Vasiliev, O. I. Medvedkov, V. G. Plotnichenko, V. V. Koltashev, A. V. Belov, M. M. Bubnov, S. L. Semjonov, and A. M. Prokhorov, "CW high power 1.24 m and 1.48 m Raman lasers based on low loss phosphosilicate fibre," *Electron. Lett.*, vol. 33, no. 18, pp. 1542–1544, Aug. 1997.

[14] M. Rini, I. Cristiani, and V. Degiorgio, "Numerical modeling and optimization of cascaded CW Raman fiber lasers," *IEEE J. Quantum Electron.*, vol. 36, no. 10, pp. 1117–1122, Oct. 2000.

[15] F. Leplingard, C. Martinelli, S. Borne, L. Lorcy, D. Bayart, F. Castella, P. Chartier, and E. Faou, "Modeling of multiwavelength Raman fiber lasers using a new and fast algorithm," *IEEE Photon. Technol. Lett.*, vol. 16, no. 12, pp. 2601–2603, Dec. 2004.

[16] K. D. Huang, X. J. Zhou, Z. J. Qin, H. C. Wu, and Z. L. Zhou, "A novel fast numerical algorithm for cascaded Raman fiber laser using the analytic approximate solution," *Opt. Commun.*, vol. 271, no. 1, pp. 257–262, Mar. 2007.

[17] Z. J. Qin, X. J. Zhou, Q. Li, H. C. Wu, and Z. L. Zhou, "An improved theoretical model of *n*th-order cascaded Raman fiber lasers," *J. Lightw. Technol.*, vol. 25, no. 6, pp. 1555–1560, Jun. 2007.

[18] M. Rini, I. Cristiani, V. Degiorgio, A. S. Kurkov, and V. M. Paramonov, "Experimental and numerical optimization of a fiber Raman laser," *Opt. Commun.*, vol. 203, no. 1/2, pp. 139–144, Mar. 2002.

[19] S. A. Babin, D. V. Churkin, A. E. Ismagulov, S. I. Kablukov, and E. V. Podivilov, "Four-wave-mixing-induced turbulent spectral broadening in a long Raman fiber laser," *J. Opt. Soc. Amer. B, Opt. Phys.*, vol. 24, no. 8, pp. 1729–1738, Apr. 2007.

[20] T. Hoshi, T. Shioda, Y. Tanaka, and T. Kurokawa, "10-Gbps DWDM transmission using multi-frequency light source with 50-GHz channel spacing," presented at the Opt. Fiber Commun./Nat. Fiber Optic Eng. Conf., San Diego, CA, Mar. 25, 2007, Paper OMS6.